LES of strong wind mechanisms at pedestrian level around buildings with same aspect ratio of 2 and different sizes

Qiang Lin [1], Yasuyuki Ishida[2], Hideyuki Tanaka[3], Akashi Mochida[4], Qingshan Yang[5], Yukio Tamura[6]

[1]Chongqing University, Chongqing, China, linqiang@cqu.edu.cn
[2]Tohoku University, Sendai, Japan, yasuyuki.ishida.e1@tohoku.ac.jp
[3]Takenaka Corporation, Tokyo, Japan, tanaka.hideyuki@takenaka.co.jp
[4]Tohoku University, Sendai, Japan, akashi.mochida.d1@tohoku.ac.jp
[5]Chongqing University, Chongqing, China, qingshanyang@cqu.edu.cn
[6]Chongqing University, Chongqing, China, yukio@arch.t-kougei.ac.jp

SUMMARY:
Large Eddy Simulations (LES) were performed to verify the type 2 variation of downwash effect reported in Tamura et al. (2019) and its influence on pedestrian-level winds around buildings. The assumption of "type 2 variation" of downwash effect, that is, pedestrian-level winds, are mainly related to wind speed change near the front stagnation level for buildings with the same aspect ratios and different sizes, is verified by analysis of pedestrian-level wind speed ratios and by examining three-dimensional flow fields around buildings by setting several control volumes (CVs) around them. The maximum mean pedestrian-level winds for buildings with the same aspect ratio of 2 are almost equal to 1.1 times the wind speed near the front stagnation level in the approaching boundary layer flow (BLF).

Keywords: Pedestrian wind environment, Downwash effect, LES

1. INTRODUCTION

Tall buildings in cities may cause uncomfortable and even unsafe pedestrian-level wind conditions. Extensive studies on pedestrian wind environments have been conducted since the 1960s. Some have mentioned the physical mechanisms of pedestrian-level strong winds around buildings, that is, downwash effect due to pressure gradient in boundary layer flow and Venturi effect due to narrowing flow sections caused by the presence of buildings (e.g., Beranek., 1984; Blocken et al., 2008), and found that downwash effect is more significant than Venturi effect for isolated high-rise buildings (Tamura, et al., 2019). Meanwhile, Tamura et al. (2019) conjectured two types of variation of downwash effect with building configurations based on measured mean pedestrian-level wind speeds around buildings: change in two-dimensional/three-dimensional flow pattern (Type 1 variation) and change in wind speed near the front stagnation height due to building sizes with the same flow pattern (Type 2 variation). Understanding of pedestrian-level strong wind mechanisms is essential to take effective measures to mitigate pedestrian discomfort and to further develop accurate and reasonable generic models (GMs) (e.g., Stathopoulos et al., 1995; Yang et al., 2022) as a fast way to predict pedestrian-level winds in the preliminary design of tall buildings. In this study, Large Eddy Simulations (LES) were performed to verify the type 2 variation of downwash effect and its influence on pedestrian-level winds for buildings with the same aspect ratio of 2 and different sizes in boundary layer flow (BLF). Accuracy of LES results was first validated by comparing them with PIV (Particle Image Velocimetry) measurements.

2. DESCRIPTION OF WIND TUNNEL EXPERIMENT

Experiments were carried out on a 1.2m-wide by 1.5m-high test section in an open-circuit boundary layer wind tunnel of Beijing Jiaotong University, China. Boundary layer flows (BLF) with a power-law exponent of 0.27 were simulated. The geometrical scale was set at 1/1000. Four square-section high-rise building models with the same width (B = 50m in full-scale) and different heights (H = 100m, 200m, 400m, 600m in full-scale), with aspect ratios (ARs) of 2, 4, 8 and 12 were tested. The flow fields around these building models were measured by a two-dimensional PIV system. Here, the measured planes of the PIV tests are shown schematically only for building models with an AR of 2, as shown in Figure 1. The measurable range of the PIV system is limited as 180m ×180m in full-scale. Coordinates are defined as x, y, and z, and the velocities of corresponding directions are denoted as u, v and w.

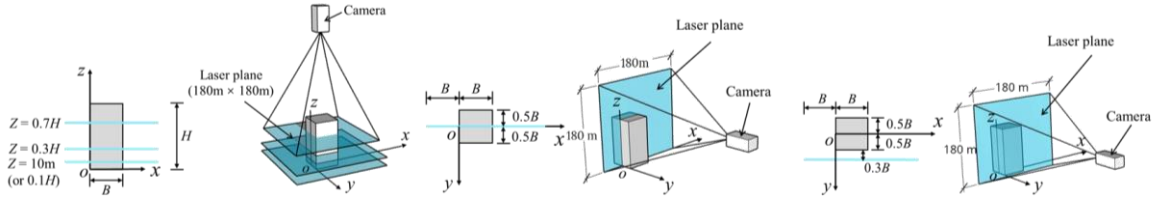

Figure 1. Measured planes for PIV test.

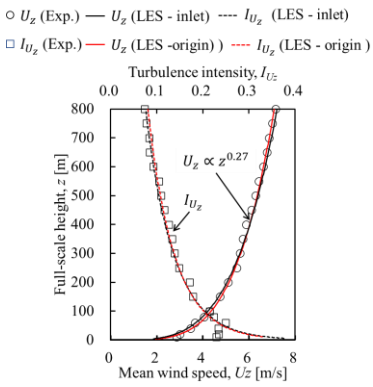

Figure 2. Boundary layer flows.

Table 1. Building configurations

AR	H/B = 2		
H (m)	H_{50}=50	H_{100}=100	H_{150}=150
B (m)	B_{25}=25	B_{50}=50	B_{75}=75

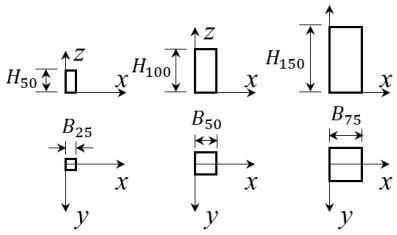

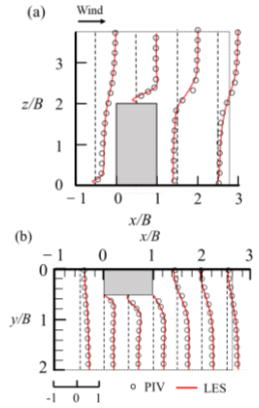

Figure 3. LES vs PIV results (a) y = 0; (b) z = 0.1H

3. NUMERCIAL SIMULATIONS

As shown in Table 1, three square-section building models were designed for LES, having the same AR of 2 and different sizes, with building heights, H: H_{50}=50m, H_{100}=100m, and H_{150}=150m, and corresponding building widths, B: B_{25}=25m, B_{50}=50m and B_{75}=75m. Table 2 lists the calculation conditions for LES. Referring to the AIJ guidelines (2019), the building width was uniformly discretized into 20 grids, and sufficient distances between building surfaces and boundaries of the computational domain were secured, in which the cross-section of the computational domain corresponds to the wind tunnel test section. The mesh stretching ratio was set to 1.08 or less. The inflow fluctuations were generated by an artificially generated method (Okaze & Mochida., 2017). Figure 2 compares the approaching flow conditions obtained from experimental and LES results in an empty computational domain and it can be seen that they show good approximation at both the inlet and the position of the building models, origin (x, y) = (0,0).

In order to validate the accuracy of the LES results, the results from PIV tests are used for comparison. Here, the comparison results for normalized mean streamwise velocities, $\bar{u}/U_{ref}$ corresponding to only a horizontal plane at $z = 0.1H$ and vertical center plane are shown in Figure 3, in which the overbar means time-average operation. $U_{ref} = 6\mathrm{m/s}$ represents the mean wind speed at 400m height in full-scale in the approaching flow. It can be seen that the mean wind velocities obtained from LES all show good approximation to those obtained from the PIV tests.

Table 1. Calculation conditions

Code	OpenFOAM v8
Computation domain	$13H(x)\times 1.2\mathrm{m}\ (y)\times 1.5\mathrm{m}\ (z)$
SGS model	WALE model
Time scheme	second-order backward
Time interval for time advancement	$1\times 10^{-4}\,\mathrm{s}$
Advection scheme	Second-order central difference (95%) + First-order upwind difference (5%)
Diffusion scheme	Second-order linear difference
Pressure solver	PISO
Outlet boundary	Advective outflow condition
Upper & side boundaries	No-slip wall
Ground & building boundaries	Spalding's law

4. SIMULATION RESULTS AND ANALYSIS

4.1 Analysis of pedestrian-level wind-speed ratios

The assumption of "type 2 variation" means that the variation of downwash effect is due to the wind speed change near the front stagnation point because of the size difference between buildings with the same AR. Therefore, the wind speed ratio, $R_{SP} = \overline{(u^2 + v^2 + w^2)^{0.5}}/U_{SP}$ normalized by the mean wind speed in the approaching flow at front stagnation level, U_{SP}, is defined. Figure 4 shows the distribution of R_{SP} at z=0.05H. It can be seen that the magnitude and distribution of pedestrian-level wind after normalizing by U_{SP} around the buildings are very similar to each other and with the same maximum of around 1.1. This result is consistent with the assumption of "type 2 variation" of downwash effect.

4.2 Flow rate analysis and the Downwash effect

In addition to the pedestrian-level wind speed ratio, the distribution of three-dimensional downwash flow fields around buildings should also be checked. Here, 15 control volumes (CVs) reflecting the downwash phenomenon around buildings are designed as shown in Figure 5(a) and the distribution of normalized mean flow rates, $Q^* = Q/Q_{ref}$ is defined and examined for convenience of comparison between different buildings, in which Q represents the mean flow rate through a surface of CVs, $Q_{ref} = (U_{SP})_{50} \times B_{50} \times 0.2H_{50}$, and $(U_{SP})_{50}$ represents the mean wind speed of the approaching flow at front stagnation level for the building with AR of 2 and width $\times$ height as $B_{50} \times H_{50}$.

Due to limited space, only the distributions of Q^* flowing from surfaces of CVs 1-5 at the fronts of the buildings are shown in Figure 5(b), in which numbers above and below the bar represent percentages of Q^* for a surface of CVs relative to the Q^* for the "front" surfaces of the CVs. For buildings of different sizes, even though the magnitude of Q^* increases with increase of building size, it can be seen that the characteristics of the flow fields around different buildings are very similar, showing almost the same percentages for surfaces of all CVs. This result verifies the

assumption on the type 2 variation of downwash effect: the same flow patterns around buildings can be assumed for buildings with the same aspect ratios.

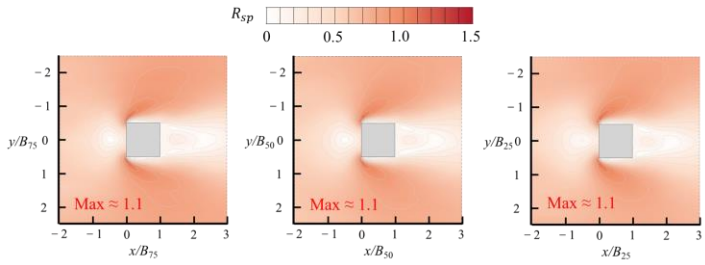

Figure 4. Distribution of R_{SP} at z=0.05H for buildings with aspect ratio 2 in BLF.

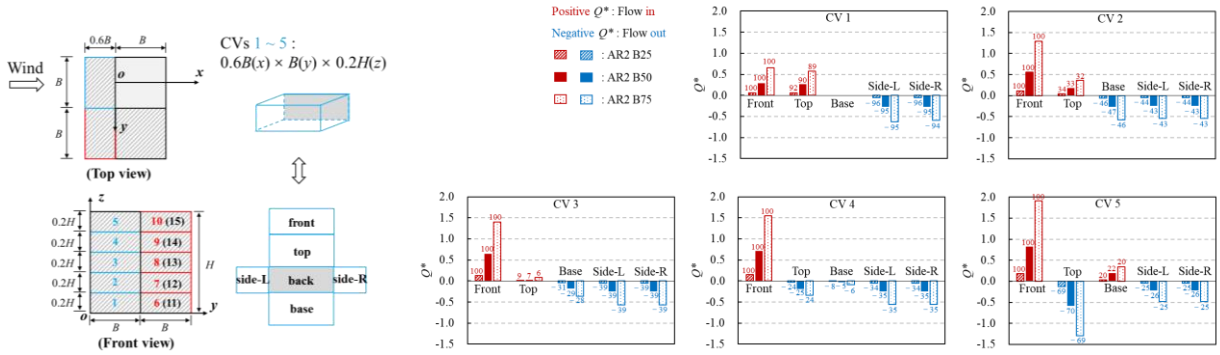

Figure 5. (a) Schematic of CVs around a building and (b) Distribution of Q^* flowing from surfaces of CVs 1-5.

4. CONCLUDING REMARKS

The assumption of type 2 variation of downwash effect is verified for buildings with the same aspect ratio of 2 and different sizes, and the maximum mean pedestrian-level winds are almost equal to 1.1 times the wind speed near the front stagnation level in BLF.

ACKNOWLEDGEMENTS

This research was partially supported by 111 Project of China (B18062, B13002), the TPU Wind Engineering Joint Usage/ Research Center Project of MEXT Japan (JPMXP0619217840) and the scholarship from China Scholarship Council (No. 202006050113). The authors are grateful for these financial supports.

REFERENCES

Beranek, W. J., 1984. Wind environment around single buildings of rectangular shape, Heron, 29(1): 1–31.

Blocken, B., Moonen, P., Stathopoulos, T., Carmeliet, J., 2008. Numerical study on the existence of the venturi effect in passages between perpendicular buildings. Journal of Engineering Mechanics, 134(12), 1021-1028.

Okaze, T., Mochida, A., 2017. Cholesky decomposition–based generation of artificial inflow turbulence including scalar fluctuation. Computers & Fluids, 159, 23-32

Stathopoulos, T., and Wu, H., 1995. Generic models for pedestrian-level winds in built-up regions. Journal of Wind Engineering and Industrial Aerodynamics, 54, 515-525.

Tamura, Y., Xu, X., Yang, Q., 2019. Characteristics of pedestrian-level mean wind speed around square buildings: effects of height, width, size and approaching flow profile. Journal of Wind Engineering and Industrial Aerodynamics, 192, 74-87.

Yang, Q., Xu, X., Lin, Q., Tamura, Y., 2022. Generic models for predicting pedestrian-level wind around isolated square-section high-rise buildings. Journal of Wind Engineering and Industrial Aerodynamics, 220, 104842.